

Evaluation of weathering effects by CIELAB color space and image analysis technique for interbedded metasedimentary rock in the northern region of Peninsular Malaysia

Mazlina Razali^{1,2}, Mohd Ashraf Mohamad Ismail¹

¹*School of Civil Engineering, Engineering Campus, Universiti Sains Malaysia, Pulau Pinang, Malaysia*

²*Civil Engineering Studies, College of Engineering, Universiti Teknologi MARA, Cawangan Pulau Pinang, Permatang Pauh Campus, Pulau Pinang, Malaysia*

Sharan Kumar Nagendran³, Zuraini Zainal³

³*Centre of Excellence for Engineering and Technology (CREaTE), Public Works Department (JKR), Alor Gajah, Melaka, Malaysia*

Hayato Tobe⁴, Kensuke Date⁵, Yasuhiro Yokota⁵

⁴*Rock Mechanics and Hydro-geology Group, Kajima Technical Research Institute, Kajima Corporation, Japan,* ⁵*Kajima Technical Research Institute, Kajima Corporation, Singapore*

Hamzah Hussin⁶

⁶*Department of Geoscience, Faculty of Earth Science, Universiti Malaysia Kelantan, Jeli, Kelantan*

ABSTRACT: Weathering process affect the engineering behavior of rock masses, reduced strength, and structural stability. In addition to the prior technology, rapid weathering evaluation by CIELAB to characterize the rock surface color. The various colors appearing on the surface of the rock slope indicated the differential weathering grades of the rock mass. UCS-Schmidt obtained by the Schmidt hammer strongly validates the color changes and can be classified into different grades. A high value in redness (a*) and yellowness (b*) indicates the rock is weathered. The results were further revealed using image analysis to confirm the analysis. The weathering zoning processed by image analysis clearly interpreted different weathering grades. This study revealed the enhanced technique as an effective tool in the preliminary evaluation of weathering effect.

Keywords: Image analysis, weathering, metasedimentary rock, CIELAB, Schmidt hammer.

1 INTRODUCTION

Weathering effects refer to the changes in physical, chemical, and biological characteristics of materials like rocks over time due to exposure to agents like temperature, water, wind, and living organisms. These effects can lead to deterioration or transformation of the rock mass, such as erosion, cracking, discoloration, and softening. Understanding weathering effects is crucial for assessing the overall state, durability, and stability of a rock mass (Tran et al., 2019). It often results in the formation of discontinuities and defect zones in rock masses, which can act as pathways for groundwater circulation. Groundwater containing chemically soluble substances can alter the color of rock surfaces, weaken their strength, and affect structural stability (Park & Kim, 2019; Tran et al., 2019). Intense chemical weathering can turn exposed rock masses into weak rocks with changed surface colors (Chung et al., 2020; Gokay, 2018). Analyzing the degree of weathering helps determine the rock's geochemical composition. Traditional methods of assessing weathering, relying on geologists' sketches, can be biased. Visual inspection can be used to evaluate rock slope stability and weathering profile characterization. Therefore, incorporating quick and descriptive weathering assessments should be a part of engineering projects involving rock masses. This study introduces a new approach using image analysis and the CIELAB color space technique to evaluate weathering

in the northern region of Peninsular Malaysia (Lee Kwan Yee et al., 2022; Yusoff et al., 2023). Digital imaging and UAV photogrammetry are employed to capture high-resolution data for detailed analysis of rock surfaces. Digital image analysis provides more accurate and efficient quantitative color measurements. DroneDeploy and UAV photogrammetry are used to generate slope outcrop images and create 3D models of the surface (Kong et al., 2021). The JudGeo Working Face software is utilized to analyze orthophoto images and identify different weathering grades based on CIELAB color data. The color of the rock surface is the primary characteristic used for differentiation, but its uniformity can vary, affecting the accuracy of observations. Weathering can also impact the mechanical properties of rock masses, further contributing to color variations. The Schmidt hammer is commonly used to assess rock strength and was employed to validate the image analysis results. This study demonstrates that incorporating novel techniques enhances traditional methods and provides valuable tools for the initial assessment of weathering effects on rock slopes.

2 GEOLOGICAL SETTING AND METHODS

2.1 Geological setting investigated region

The weathered metasedimentary rock in the northern region of Peninsular Malaysia is found along Federal Route 175, about 800m from Gubir Dam, Sg Muda. This area mapped using DroneDeploy covers 1.45 acres with a vertical length of 68.71m and a horizontal length of 48.32m (Figure 1). It is part of the Semanggol Formation in the Sik District of Kedah State, previously believed to be Triassic shale but now identified as altered to schist or phyllite. The research area consists of sedimentary and metasedimentary rock, including sandstone, shale, quartzite, and schist. Fossils from the early Jurassic period have been found in the red conglomerate and mudstone of the Saiong Beds near Muda Dam and Gubir areas (Hutchison & Tan, 2009). The investigation at the Muda Dam site revealed a sequence of sedimentary rocks ranging from fine-grained mudstones to coarse-grained pebbly sandstone.

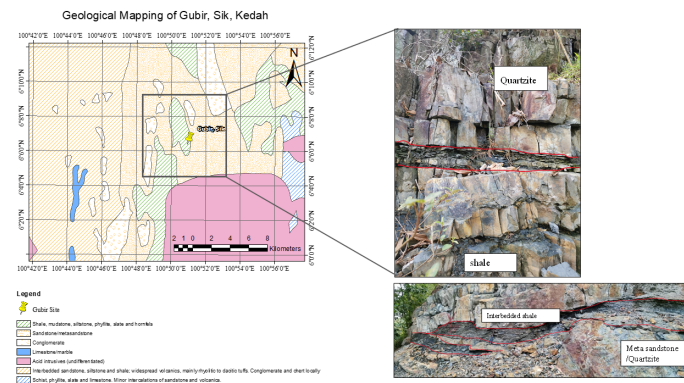
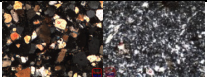
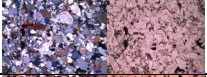

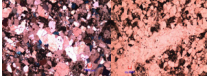


Figure 1. Geological mapping of the studied region.

The investigation revealed that the main rock type in the study area was tightly compacted quartzite, with occasional thin layers of mudstone. Detailed examination of hand specimens confirmed the rock's fine-grained texture, mostly grey in color, consisting primarily of mica and quartz fragments. A comparison of grain size and mineral composition between quartzite, sandstone, and shale showed distinct differences resulting from metamorphism. X-ray powder diffraction analysis indicated that quartzite samples contained quartz, hematite, muscovite, and minor amounts of other minerals, while shale samples consisted of quartz, muscovite, and various clay minerals. These findings indicate that the study area consists of alternating layers of metasedimentary sandstone (or quartzite) and shale. The dominant weathered rock types in the slope profile range from Grade II to V, with quartzite and sandstone being the most common.

Table 1. Typical petrographic image analysis with Crossed Polarized Light (CPL) image and Plain Polarized Light (PPL) image for quartzite, quartz sandstone, pebbly sandstone, and shale (scale photograph 1: 1000 μ m).

Type of Rocks	Mineral Composition		Photograph
	TS	XRD	
Quartz Sandstone	Quartz	Quartz, Muscovite, Chromian	
Quartzite	Quartz	Quartz, Illite, Hematite, Muscovite, Anatase, Kaolinite, Illite and Sanidine.	
Shale/mudstone	Quartz	Quartz, Sericite, Kaolinite, Illite, Muscovite, Kaolinite, Clinocllore and Rutile.	
Pebbly Sandstone	Quartz Vein Rock Fragment	Quartz, Muscovite, Kaolinite, Illite and Sanidine.	

2.2 Weathering mechanism and integration of CIELAB color space with image analysis

These studies highlight the significance of pyrite in the chemical weathering of soft sedimentary rocks like mudstone or shale. The aim of this paper is to explain the process of chemical weathering and its impact on the mechanical properties of coarse-grained sandstone with some clay in a humid mountainous region. In hot and humid climates, distinct weathered profiles form with different zones exhibiting physical, chemical, or mineralogical variations. Field investigations discovered failures in the weathered quartzite-sandstone across all weathering horizons. The weathering profile of this interbedded metasedimentary rock is depicted in Figure 2, analyzed through color, petrographic thin section, and X-ray Powder Diffraction techniques. It is divided into three zones: bedrock, intermediate, and residual soil. Fig. 2 also displays field photographs of zones A, B, and C, with different characteristics. CIELAB, derived from Hunter's Lab, is a color space that accurately represents perceptual differences between colors. Using CIELAB color space in image processing algorithms yields more precise results. The L^* , a^* , and b^* values of the rock slope were measured using a colorimeter (Figure 3a and 3b) to establish a correlation between weathering grade and color changes. The L-type Schmidt hammer (Figure 3c) was used to determine the in-situ uniaxial compressive strength (UCS-Schmidt) of rock samples. Data collection involved using both hands for accuracy, resulting in 150 measurement points. UAV photogrammetry and image analysis techniques were employed to capture detailed outcrop images of the slope and analyze its geological structure and composition. The workflow for image analysis is illustrated in Figure 4.



Figure 2. Weathering profile for the study area.



Figure 3. Insitu testing; a) Colorimeter testing device, b) methods to setting up the colorimeter, c) validation results using L-type Schmidt hammer.

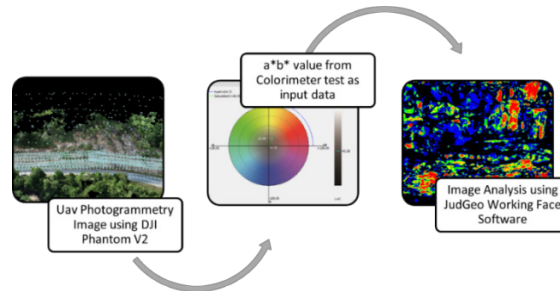


Figure 4. Workflow of processing images in JudGeo working face software (Tobe et al., 2018).

3 RESULTS AND DISCUSSION

3.1 Weathering effects using $L^*a^*b^*$ value (CIELAB)

The rock slope color indicates weathering degree. To illustrate the correlation between weathering degree, a^* , b^* values, and rock color, measurement points No. 34 and No. 3 were selected (Fig. 5a and 5b). As weathering increases, rock color becomes yellowish, darker, or reddish, with corresponding increases in a^* and b^* values. No. 34 represents unweathered rock (Grade II-I), while No. 3 is slightly weathered (Grade IV-III). The a^*b^* value was validated by UCS results from Schmidt hammer testing.

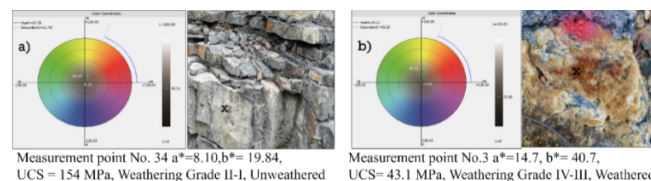


Figure 5. Typical correlation of rock slope surface color with UCS-Schmidt at investigated region; a) Unweathered, original colour of gray sandstone, b) Weathered, oxidation zone (kaolinite).

Color changes involve oxidation. Fig. 6 depicts the correlation between ab values of typical data after removing outliers. The figure shows that increased ab values result in a yellowish rock surface coloration ($R^2 > 0.8$). Pyrite oxidation is a significant mineralogical change in the oxidation zone, commonly found in gray and green sandstones (point No. 64). It produces sulfuric acid and iron oxide or hydroxide, altering the rock's color to yellowish or reddish. Iron-oxidizing bacteria, like *Thiobacillus ferrooxidans*, facilitate pyrite oxidation, detected in oxidation fronts. Birnessite in phyllite, a type of layered manganese oxide (point No. 13), forms through weathering of manganese minerals or bacterial oxidation. Sanidine in metasandstone (point No. 76) can undergo chemical weathering, transforming into clay minerals like kaolinite and smectite when exposed to water and oxygen. Chlorite oxidation in mudstone/shale yields smectite in the oxidized zone. Feldspar alters, releasing aluminum and silica ions, reacting with water to form kaolinite. Kaolinite, typically found in tropical regions, exhibits yellowish and white a^* values (Fig. 6, points No. 12 and 49).

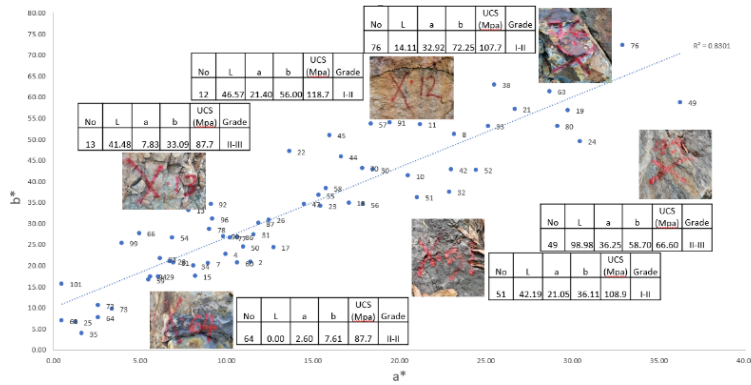


Figure 6. Correlation of a*b* values with onsite photographs.

3.2 Weathering effects using Image Analysis

The rock weathering gradation was determined using JudGeo's working face software. In Fig. 7, black (14%) and blue (28%) areas indicate weathering grade I-II, while approximately 33% coverage of green corresponds to weathering grades III-IV. The rock slope exhibits weathering grades IV-V, with 9% yellow and 4% orange color coverage. Yellow, orange, and red colors (12%) indicate rock decomposition into soil, with red representing vegetation. The simulated input data for a*b* values range from 2 to 20. Vegetation in the soil can loosen rock masses. Analyzing the rock mass allows quantitative determination of potential failure mechanisms. Slump slides occur in Grade VI weathered rock, transitioning from steep at the head to flat at the toe, indicating a transition to soil. Debris flow can occur in Grades V and IV, with fragmented rock and water-laden soil rushing down mountainsides. Weakened outer rock causes rolling rocks on Grades III and II, leading to rockfall, block glides, and landslides. Plane failure occurs in Grade I, characterized by a straight stress crack separating two portions on an inclined plane. De Freitas et al., (2009) established a weathering gradation scheme from Grades I to VI, where Grade I rock is stronger than Grade VI due to weathering weakening. Marinos, (2017) assigned rock grades R0 to R6, with R6 indicating the highest strength and R0 the lowest. Higher UCS values obtained with the Schmidt hammer correspond to low weathering grades (Aydin, 2015).

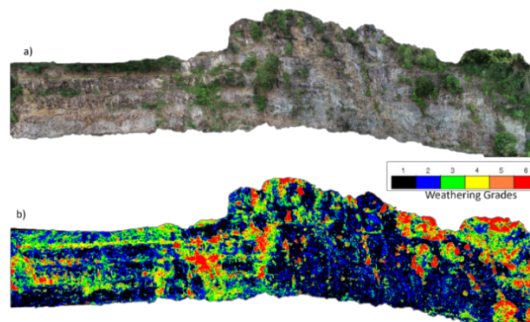


Figure 7. (a) Outcrop of the Gubir slope; (b) Final result of the image analysis for the Gubir slope.

4 CONCLUSION

In mining and civil engineering projects, it's important to understand the properties of rocks on or within the project sites. This study focused on analyzing the color differences between unweathered and weathered rock surfaces. Weathered rock zones often indicate weaker stability and discolored areas on the rock surface. The color analysis revealed that as different types of weathering occur, the fresh rock surfaces become discolored. Chemical and biological weathering are significant factors contributing to the discoloration of the rock surface. Comparing unweathered and weathered rock

surfaces showed differences in color analysis data. Areas with high redness (a*) and yellowness (b*) indicated different mineral content compared to darker areas. The CIELAB color surface method proved to be effective in analyzing colors. Image analysis was found to be a cost- and time-effective approach for studying weathered slopes. However, it is recommended to conduct additional tests on different rock slope locations to ensure accurate analysis and minimize the risk of misjudging a slope based solely on surface weathering. This investigation specifically focused on a metasedimentary rock in the northern region of Peninsular Malaysia.

ACKNOWLEDGMENTS

We thank Centre of Excellence for Engineering and Technology (CREaTE) for their financial support for the fieldwork on the topic "Development of Rapid Quantitative Assessment for Weathered Rock Slope in Tropical Region using the Integrated Image Analysis Technique" (grant no. 304.PAWAM.6050482.J111). We are also grateful to Kajima Technical Research Institute Japan and KATRIS for sharing their knowledge and resources. Additionally, we acknowledge the anonymous reviewers for their valuable feedback and suggestions that improved the manuscript.

REFERENCES

- Aydin, A. (2015). The ISRM Suggested Methods for Rock Characterization, Testing and Monitoring: 2007-2014. *The ISRM Suggested Methods for Rock Characterization, Testing and Monitoring: 2007-2014, 2007–2014*. <https://doi.org/10.1007/978-3-319-07713-0>
- Chung, H. Y., Jung, J., Lee, D. H., Kim, S., Lee, M. K., Lee, J. Il, Yoo, K.-C., Lee, Y. Il, & Kim, K. (2020). *minerals Chemical Weathering of Granite in Ice and Its Implication for Weathering in Polar Regions*. <https://doi.org/10.3390/min10020185>
- De Freitas, M. H., Hack, H. R. G. K., Higginbottom, I. E., Knill, J. L., & Maurenbrecher, M. (2009). Engineering geology: Principles and practice. In *Engineering Geology: Principles and Practice*. <https://doi.org/10.1007/978-3-540-68626-2>
- Gokay, M. K. (2018). Analyses of Rock Surface Colour Changes Due To Weathering. *Selcuk University Journal of Engineering ,Science and Technology*, 6(1), 1–13. <https://doi.org/10.15317/scitech.2018.111>
- Hutchison, C. S., & Tan, D. N. K. (Eds.). (2009). *Geology of Peninsular Malaysia*. Murphy.
- Kong, D., Saroglou, C., Wu, F., Sha, P., & Li, B. (2021). Development and application of UAV-SfM photogrammetry for quantitative characterization of rock mass discontinuities. *International Journal of Rock Mechanics and Mining Sciences*, 141, 104729. <https://doi.org/10.1016/J.IJRMMS.2021.104729>
- Lee Kwan Yee, A., Razali, M., Ismail, M. A. M., Yusoff, I. N., Nagendran, S. K., Zainal, Z., Tobe, H., Date, K., & Yokota, Y. (2022). Preliminary analysis of rock mass weathering grade using image analysis of CIELAB color space with the validation of Schmidt hammer: A case study. *Physics and Chemistry of the Earth, Parts A/B/C*, 103291. <https://doi.org/10.1016/J.PCE.2022.103291>
- Marinos, P. V. (2017). Geological Behaviour of Rock Masses in Underground Excavations. *Bulletin of the Geological Society of Greece*. <https://doi.org/10.12681/bgsg.11300>
- Park, J., & Kim, K. (2019). Quantification of rock mass weathering using spectral imaging. *Journal of the Southern African Institute of Mining and Metallurgy*, 119(12), 1039–1046. <https://doi.org/10.17159/2411-9717/708/2019>
- Tobe, H., Miyajima, Y., Shirasagi, S., Yamamoto, T., & Kawabata, J. (2018). A rapid image analyzing method for determining crack distribution and interval on tunnel faces. *ISRM International Symposium - 10th Asian Rock Mechanics Symposium, ARMS 2018*.
- Tran, T. V., Alkema, D., & Hack, R. (2019). Weathering and deterioration of geotechnical properties in time of groundmasses in a tropical climate. *Engineering Geology*, 260(January), 105221. <https://doi.org/10.1016/j.enggeo.2019.105221>
- Yusoff, I. N., Mohamad Ismail, M. A., Tobe, H., Date, K., & Yokota, Y. (2023). Quantitative granitic weathering assessment for rock mass classification optimization of tunnel face using image analysis technique. *Ain Shams Engineering Journal*, 14(1), 101814. <https://doi.org/10.1016/J.ASEJ.2022.101814>